Journal of Power Sources 180 (2008) 760–766

Contents lists available at ScienceDirect

Journal of Power Sources

journal homepage: www.elsevier.com/locate/jpowsour

Gas selectivity measurements as a diagnostic tool for fuel cells

Sumit Kundu, Michael W. Fowler*, Leonardo C. Simon

Department of Chemical Engineering, University of Waterloo, 200 University Avenue West, Waterloo, Ontario, Canada N2L 3G1

ARTICLE INFO

Article history:
Received 30 January 2008
Received in revised form 20 February 2008
Accepted 21 February 2008
Available online 4 March 2008

Keywords:
Fuel cell
Membrane selectivity
Crossover
Degradation mode
Diagnostic

ABSTRACT

In this study, gas permeability and selectivity measurements are used to identify when membrane thinning or integrity failures have occurred in a fuel cell membrane electrode assembly and hence be used as a tool to identify when chemical or mechanical degradation is the dominant mode of failure. A fuel cell was operated at open circuit voltage conditions and the permeability of five different gasses (H_2, He, N_2, O_2, Ar) were measured periodically. The results showed that through a fresh MEA the gasses permeated via a solution diffusion type mechanism though after 150 h of degradation the permeation behaviour changed to Knudsen diffusion mechanism. This was interpreted to indicate that an integrity failure had occurred in the ionomer membrane. Voltage data also shows an increase in voltage degradation rate after 150 h and a drop in polarization performance. Furthermore, there was an increase in fluoride emission rate. Analysis of the de-catalyzed membrane after degradation revealed rips and tears in the ionomer membrane and no significant thickness changes.

1. Introduction

Fuel cells are a promising alternative energy technology that promotes lower urban air pollution and increased energy security. Some of the current drawbacks of polymer electrolyte membrane (PEM) fuel cell technology are durability issues with materials and system components. The polymer electrolyte membrane in a fuel cell is one such component that is susceptible to a variety of degradation modes ranging from chemical, mechanical, and thermal degradation [1,2]. The different causes of polymer electrolyte membrane degradation range from manufacturing, design, and assembly issues such as compression or membrane thickness variability [2], failure caused by material properties such as swelling and failure from the operational conditions such as high and low humidity or freezing conditions [3–5]. Mathias et al. [6] and LaConti et al. [1] provided detailed reviews of different failure modes of PEM fuel cells as a whole. Since the polymer electrolyte is responsible for transporting protons, water, and acting as a gas barrier within the fuel cell, its failure results in the failure of the entire fuel cell.

When the electrolyte degrades from fuel cell operation, a common observation is membrane thinning caused by chemical degradation [7,8], development of rips and tears from mechanical degradation [9,10], or some combination of the two since both failure modes may be present at the same time. In an effort to understand chemical and mechanical degradation separately, accelerated durability experiments have been developed to specifically target them. Chemical degradation has been typically studied with open circuit voltage (OCV) durability experiments [11–13] while mechanical degradation is often studied by hydration cycling [6,14]. Irrespective of which accelerated durability experiment is used or even if no specific accelerated test protocol is applied during testing, one of the main measures of the rate of degradation or indicator of failure is the crossover flow rate. This measurement typically involves pressurizing one side of the cell and measuring the flow rate of the gas (often hydrogen or nitrogen) on the opposite side [15]. Hydrogen crossover has also been measured electrochemically using a hydrogen pump experiment [13] though it is similar in nature to the manual measurement. The benefit of this diagnostic test is that it is easy to perform, easy to interpret the results, and straightforward to create failure criteria based on it. Unfortunately, this measurement has some issues that limit its usefulness as a research tool.

One such weakness is that crossover measurements are not sensitive to the mode of degradation. Gas crossover will increase during an OCV durability experiment (thought to promote chemical degradation) and from hydration cycling experiments (thought to promote mechanical degradation). In tests designed to accelerate one degradation mode, changes in crossover can generally be attributed to that particular mode. However, it is not as straightforward to distinguish the dominant mode of degradation, leading to increased crossover, in a more generic durability experiment where no single mode is targeted. To the author's knowledge, there are no test protocols in the literature that are able to distinguish between

* Corresponding author. Tel.: +1 519 888 4567x33415; fax: +1 519 746 4979.
E-mail addresses: s2kundu@uwaterloo.ca (S. Kundu), mfowler@uwaterloo.ca (M.W. Fowler).

0378-7753/$ – see front matter © 2008 Elsevier B.V. All rights reserved.
doi:10.1016/j.jpowsour.2008.02.050

the two modes. However, as will be shown, with the measurement of crossover rates of multiple gas species it is possible to create a diagnostic test that distinguishes when chemical degradation is dominant and when mechanical failure has occurred.

In this study, an OCV durability test was employed to degrade a membrane electrode assembly in situ. Gas crossover measurements were conducted periodically throughout the durability test using five test gasses: hydrogen, helium, nitrogen, oxygen, and argon. The crossover measurements were used to determine how gas selectivity changed with time and these results were used to determine if membrane thinning, or mechanical rips and tears, were the primary type of failure. It is proposed that selectivity measurements can be a simple and valuable method of distinguishing between membrane thinning and mechanical failure and thus can help distinguish if chemical or mechanical degradation is the dominant mode leading to cell failure. The analysis of the selectivity curves was then compared with open circuit voltage measurements, fluoride release rates, and SEM images of the degraded membrane.

1.1. Membrane defects and selectivity

Gas transport thorough membranes can be broadly described by Fick's law as shown in Eq. (1). P_M is the membrane permeability, p_I and p_{II} are the partial pressures of the gas of interest on either side of the membrane, N_A is the flux of the gas species across the membrane of thickness (δ).

$$N_A = \frac{P_M(p_I - p_{II})}{\delta} \quad (1)$$

At constant relative humidity the permeation behaviour has been found to follow Fick's law [16] and the value of P_M depends on the type of permeation behaviour. For solution diffusion type behaviour, which is common for solid polymer membranes such as Nafion™, the permeability is related to the permeating gas and factors such as the molecular size, solubility, and affinity to the substrate [17]. In the case of Nafion™ 117 the permeability was measured for five different gasses by Chiou and Paul [18] who found that the order of gasses from most permeable to least permeable was He, H_2, O_2, Ar, and N_2. Inspection of Eq. (1) shows that if a membrane thins during chemical degradation (assuming no significant change in the permeability coefficient) the gas flux through the membrane (crossover rate) will increase.

In porous membranes, such as the catalyst layer of a fuel cell, the gas flux can be described using Knudsen theory. Knudsen behaviour is valid for gasses diffusing though porous materials where the pore size is less than the mean free path of the molecule. Eq. (2) describes the gas flux across a porous membrane. N_A is flux, M is the molecular weight of the permeate gas, T is the temperature, ε represents the porosity, r is the mean radius of the pores, and R is the ideal gas constant. Generally, transport through pores is much faster than diffusion through a membrane by the solution diffusion mechanism. Comparison to Eq. (1) shows that the permeability coefficient when Knudsen transport dominates will be linearly related to $M^{-1/2}$.

$$N_A = \frac{4}{3} r\varepsilon \left(\frac{2RT}{\pi M}\right)^{1/2} \frac{(p_I - p_{II})}{\delta RT} \quad (2)$$

Gas selectivity of gas A to gas B, α_{AB}, can be defined using Eq. (3).

$$\alpha_{AB} = \frac{N_A}{N_B} \quad (3)$$

In the case of Knudsen diffusion this reduces to Eq. (4).

$$\alpha_{AB} = \frac{N_A}{N_B} = \frac{\sqrt{M_B}}{\sqrt{M_A}} \quad (4)$$

A solid polymer membrane that normally exhibits solution diffusion transport behaviour may change to Knudsen behaviour with the development of defects. Takahashi et al. [19] used this behavioural change to study the effects of irradiating PET with heavy ions by measuring the permeability of several gasses before and after the process. They found that the permeability of gasses through the fresh polymer membrane showed no trend with the molecular weight of the permeate and after irradiation the gas permeability showed an increasing trend with $M^{-1/2}$. Other works have modeled membranes with defects as having a combined contribution from solution diffusion and Knudsen diffusion such as the solution diffusion imperfection model [20,21]. This technique may also be applied to fuel cells to identify thinning phenomena and the onset of mechanical failure. This type of diagnostic test could then be used to evaluate the extent to which each type of degradation is important and then draw some conclusions on which degradation modes are most dominant in the given fuel cell configuration and conditions.

2. Experimental

Fuel cell experiments used 10 cm^2 fuel cell hardware built in-house with a single pass serpentine flow path. The ionomer membrane used was Nafion™ 112 and used cloth gas diffusion electrodes on the anode and cathode. Open circuit voltage experiments used hydrogen and air and their flow rates were controlled with mass flow controllers from Omega. The flow rates were maintained at 140 ml min^{-1} for hydrogen flow and 400 ml min^{-1} of air flow. The gas streams were humidified using Perma-Pure hydrators before entering the fuel cell. The cell was operated in an oven which was maintained at 80 °C. The relative humidity of the reactants was 80%. When measuring polarization performance, cell stoichiometry was maintained at 1.2 and 2 for the anode and the cathode, respectively.

Fluoride ion analysis was carried out by fluoride ion chromatography with a Dionex ED40 electrochemical detector working with a Dionex GP40 gradient pump. The minimum detectable fluoride ion concentration is 0.011 ppm F^-.

SEM analysis used a LEO SEM with field emission Gemini Column. X-ray compositional analysis was done using an electron dispersive spectroscopy (EDS) manufactured by EDAX. The detection limit of the EDAX system is atoms with atomic weights equal to or larger than carbon. Samples catalyst coated membrane (CCM) were cut into squares of approximately 0.5 cm × 0.5 cm and fixed to an aluminium stub with double-sided conductive tape. Cross-sections were made by freeze fracture from a strip of sample submerged in liquid nitrogen. Once frozen, the sample was broken in half while still submerged. Samples were also sputter coated with gold to improve conductivity. The gas diffusion electrode (GDE) was removed from the ionomer membrane by applying methanol to the membrane electrode assembly. This allowed easy removal of the GDE with no trauma to the ionomer membrane.

Permeability was measured with the assembled fuel cell. Both the anode and cathode sides were first purged with the test gas (H_2, He, N_2, O_2, Ar). Once purged the anode side was pressurized to 3–6 psi of the test gas. The cathode side was closed and the pressure was monitored with time. The permeability of each of the gasses through the membrane was determined by fitting Fick's law to the cathode pressure data.

Gas permeation in a fuel cell membrane electrode assembly is not as simple as that for simple membranes as found in the literature. In fuel cells, the gas molecules must be transported through the porous anode gas diffusion layer, anode catalyst layer, then through the electrolyte membrane, followed by the cathode cat-

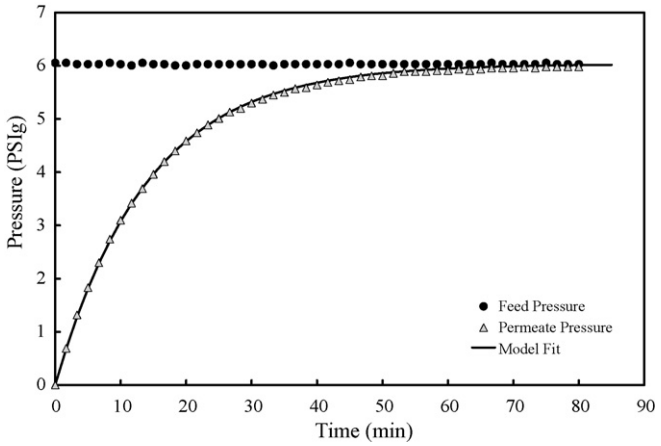

Fig. 1. Typical pressure versus time data for permeability testing as well as the model fit to the permeate pressure curve.

alyst and gas diffusion layers. A simplifying assumption made for this study is that the electrolyte membrane limits the gas permeation rate in a fresh membrane and as such, the ionomer thickness was used in calculations. It is further assumed that the permeability through the bulk polymer membrane, P_M, of gasses through the ionomer does not change with degradation. Furthermore, a change in crossover rate is considered to have two causes, the development of holes in the membrane or membrane thinning.

Since it is not feasible to measure the ionomer membrane thickness over the course of the testing, permeability data reported at different cell ages are apparent permeability, P^*, which is calculated from Eq. (5) using the thickness of the fresh membrane, δ^0. Changes in the apparent permeability offer insight into changes in the mechanism of permeation as well as changes in ionomer membrane thickness. The relation between apparent permeability, bulk permeability, and membrane thickness is given in Eq. (6). A change in the bulk permeability, P_M, from solution diffusion type to Knudsen type will have a corresponding effect on the apparent permeability, while a decrease in membrane thickness, δ_t, will be seen as an increase in apparent permeability while maintaining the characteristics of a solution diffusion transport mechanism.

$$N_A = \frac{P^*(p_I - p_{II})}{\delta^0} \quad (5)$$

$$P^* = P_M \frac{\delta^0}{\delta_t} \quad (6)$$

3. Results

3.1. Gas permeability of fresh and aged MEAs

Initial gas permeability measurements for four gasses, He, H_2, Ar, and N_2 was measured for the MEA at the beginning of life (oxygen was not initially measured). Gas permeability was estimated from permeate pressure versus time data for which a typical measurement is shown in Fig. 1. Permeate pressure initially increases linearly and then the rate of increase begins to decay as the permeate pressure approaches the feed pressure. There is no observable lag time since initially both the feed and permeate sides of the fuel cell contain atmospheric pressures of the test gas. As such, solubility and diffusivity cannot be garnered from this data, however this limitation does not impact the diagnostic technique being proposed.

The initial permeability measurements are shown in Table 1. The order of permeability of the four measured gasses are

Table 1
Initial permeability of various gasses through a fresh MEA

Gas	Permeability (Barrers)	Selectivity w.r.t. H_2	Radius (pm)
He	0.2491	2.00	31
H_2	0.1248	1.00	74
O_2	–	–	150
Ar	0.0570	0.19	71
N_2	0.0242	0.46	146

$He > H_2 > Ar > N_2$. This result is consistent with other permeability studies [18] which reported the same order of gas permeability for Nafion^{TM} membranes and generally follows a trend with molecular size of the molecules. This result also serves as confirmation that the electrolyte membrane is the controlling factor in permeation through the fresh membrane. The results show that through the fresh MEA helium is twice as permeable (selective) as hydrogen and both of these species are an order of magnitude more permeable than argon, which is more permeable than nitrogen through the fresh membrane.

Aging of the membrane was carried out using an open circuit voltage (OCV) durability test. The cell ran for a total of 300 h and was stopped after 156 h and 300 h for gas permeability and polarization curve measurements, respectively. Additionally, hydrogen and helium permeability measurements were done after 68 h of operation. Plots of gas permeability with time for each of the gasses are shown in Fig. 2a–e. Gas permeability increased exponentially with time showing typical behaviour when compared to gas crossover measurements in the literatures [4,14]. The onset of the increasing trend is after 156 h of operation for each of the gasses. This indicates that some event may have occurred, or accelerated, at that point in the testing. An interesting feature of these plots is that the order of permeability has changed. At the end of the experiment the permeability of hydrogen is the highest out of all the gasses followed by helium. Furthermore, the permeability of nitrogen surpasses that of argon after long degradation times.

Plots of apparent permeability versus the inverse square root of molecular weight ($M^{-1/2}$) are shown for the fresh membrane in Fig. 3a and for the membrane at different ages in Fig. 3b. The plot of the apparent permeability results for the fresh membrane show no trend with $M^{-1/2}$ which is consistent with prior classification of diffusion through the membrane taking place via a solution diffusion mechanism. However, measurements after 150 h and 300 h all show an increasing trend with $M^{-1/2}$ which is indicative of Knudsen flow across the MEA. This is likely due to integrity failures in the membrane. One possibility is that the presence of small pinholes in the polymer or other imperfections changing the permeability characteristics of the membrane. Another possibility is that the membrane suffered a larger failure such as a tear. In this second case the ionomer membrane will no longer limit gas permeation. Instead, the catalyst layer and/or gas diffusion layer will become limiting. Due to the porous nature of those layers, the permeation behaviour will be of Knudsen type. The slope of the curves also become steeper with fuel cell age. This can be caused by a variety of effects such as an increase in the size of the failure or an increase in the number of failures with time in the membrane electrolyte. From this data, estimates of number and size of the defects cannot be determined.

The data in Fig. 3 indicates that after 156 h the membrane has lost mechanical integrity and that a hole or rip must have formed. Gas selectivity measurements versus time for different gas pairs are able to show when diffusion changed from solution diffusion to Knudsen more clearly. A plot of selectivity with time for helium and hydrogen is shown in Fig. 4. The results show that He/H_2 selectivity decreases almost immediately. Between 0 h and 120 h, the selectiv-

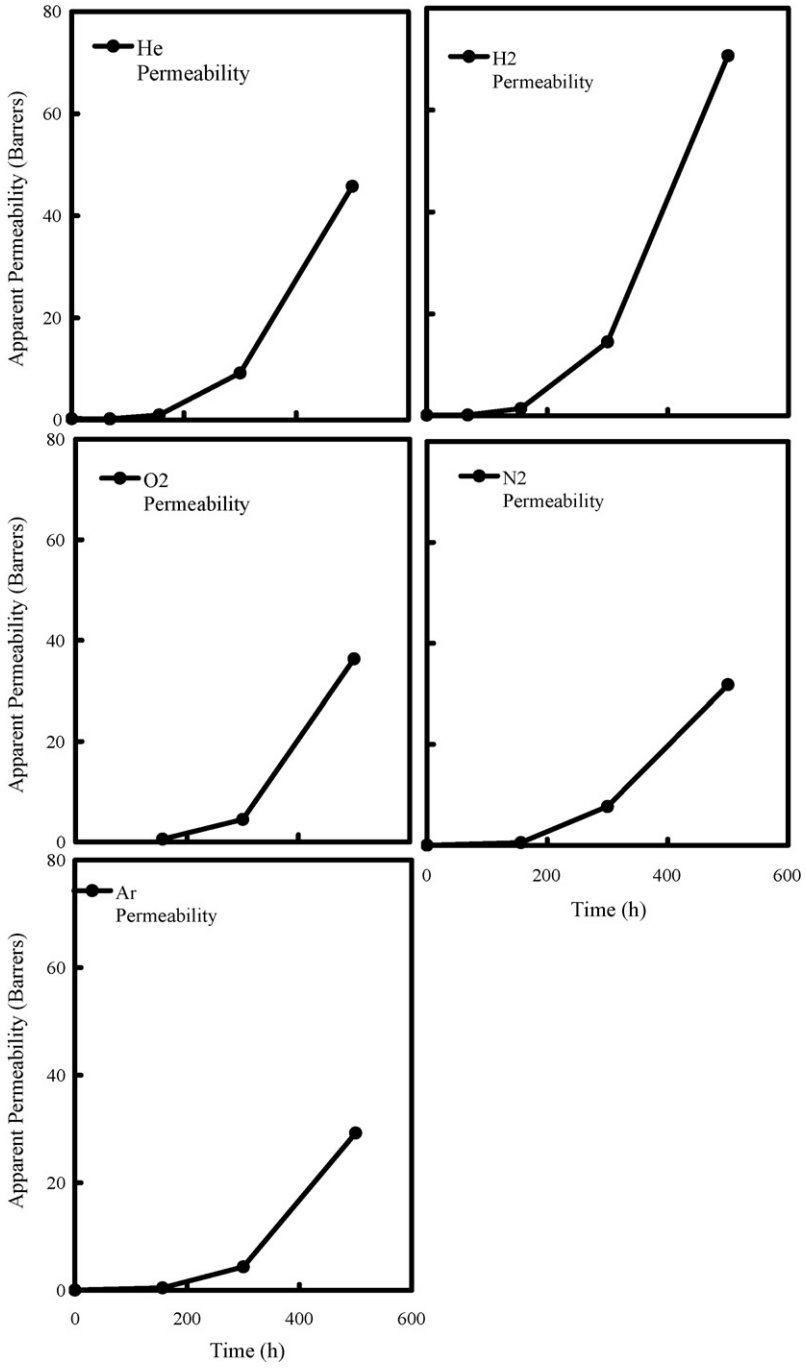

Fig. 2. Apparent permeability with time for various gasses.

ity approaches Knudsen theory predictions. During that time small integrity failures may have developed in the membrane creating a period of time where both diffusion through the membrane and diffusion through these small tears contributed to overall crossover and the increase in apparent permeability. After 120 h the selectivity stabilizes and resembles Knudsen theory predictions. This implies that a negligible amount of the increase in crossover was further caused by membrane thinning. Selectivity of other gas pairs showed similar trends though some deviated from final values predicted by Knudsen theory. These deviations are attributed to small measurement errors, especially for the gasses that were the least permeable. Overall, these results indicate that despite using an accelerated test for chemical degradation of fuel cell materials, mechanical failure of the membrane is the primary cause of failure in this test.

3.2. Open circuit voltage measurements and polarization behaviour

With consideration of the clear changes in apparent permeability and selectivity behaviour it is of interest examine the effect on performance. Open circuit voltage and polarization curve measurements were taken during the testing period. OCV data, Fig. 5, shows many similar trends with other such data sets including a transient recovery phenomenon after polarization curve measurement. In the first degradation segment, the voltage initially decays before

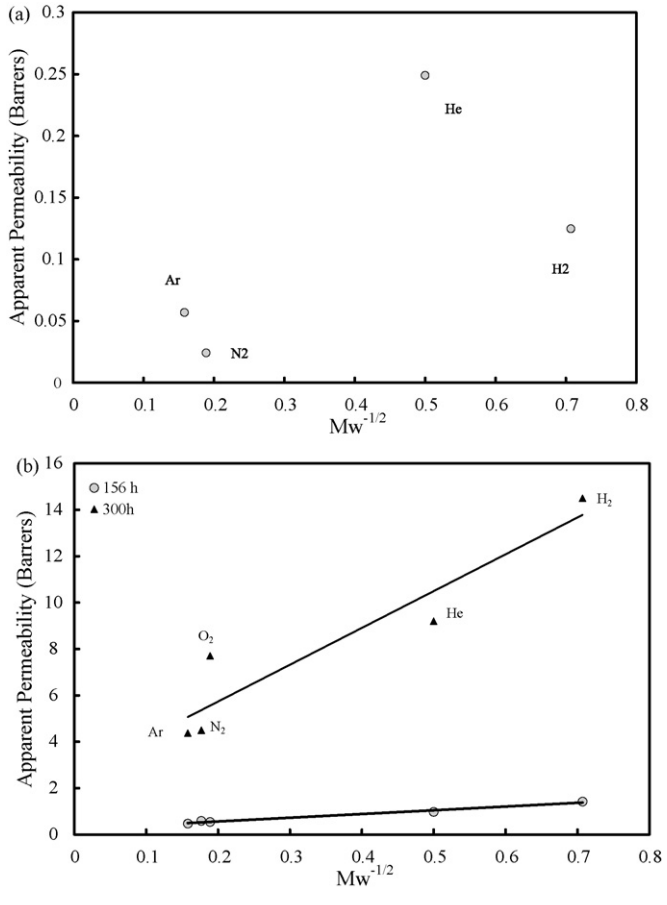

Fig. 3. Apparent permeability versus $M_w^{-1/2}$ for different gasses at different times (a) 0 h, (b) 156 h and 300 h.

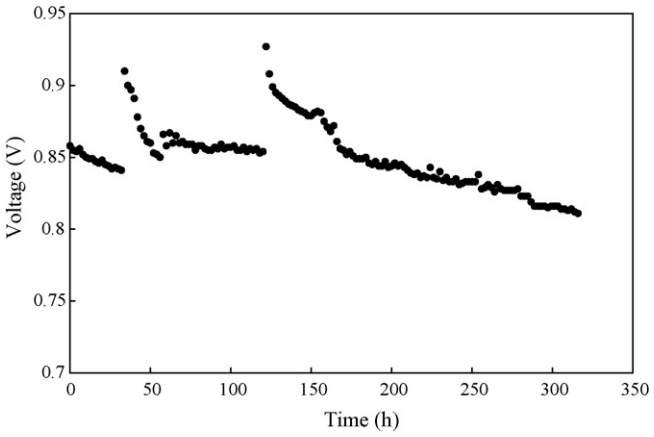

Fig. 5. Open circuit voltage data over the testing period.

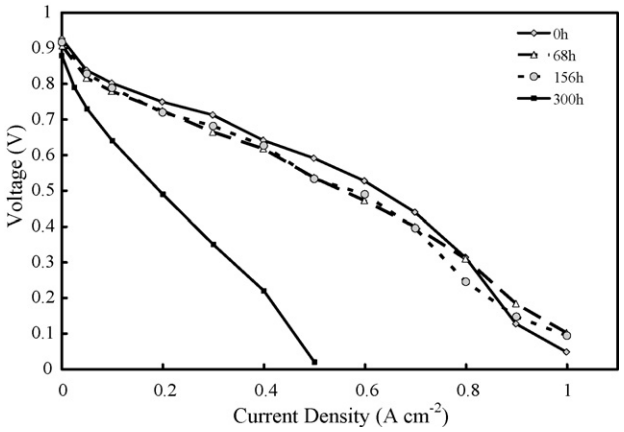

Fig. 6. Polarization curves at different ages of the membrane.

stabilizing. Once interrupted at 68 h the voltage again decays but stabilizes at approximately 0.86 V, slightly higher than the end of the first segment. After 156 h the voltage continually degraded until testing was concluded. The voltage degradation rate can be seen to increase at approximately the same time as the onset of Knudsen diffusion through the membrane. This also coincides with a dramatic increase in crossover rate (Fig. 2).

The change in fuel cell performance is more evident in the polarization curve measurements. Polarization curve measurements, Fig. 6, show that up to 150 h of operation, performance curves are similar, indicating minimal degradation. This is especially interesting since crossover during the time leading up to 150 h increased by a factor of 10. However, the polarization curve at 300 h shows a very significant drop in performance. Permeability between 150 h and 300 h increased by another factor of 10, or 100-fold from beginning of life and is consistent with an integrity failure.

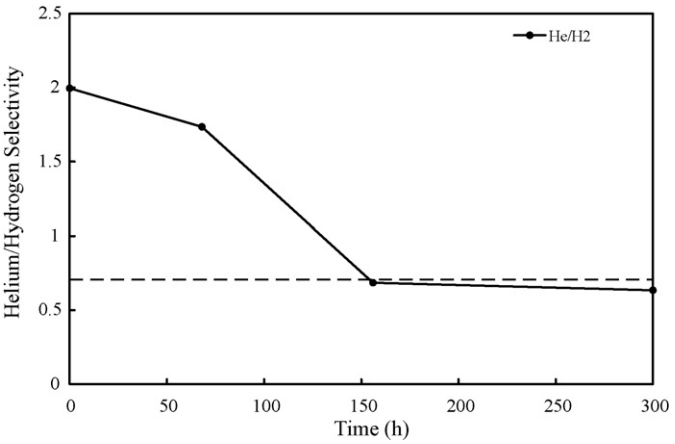

Fig. 4. He/H_2 selectivity with time.

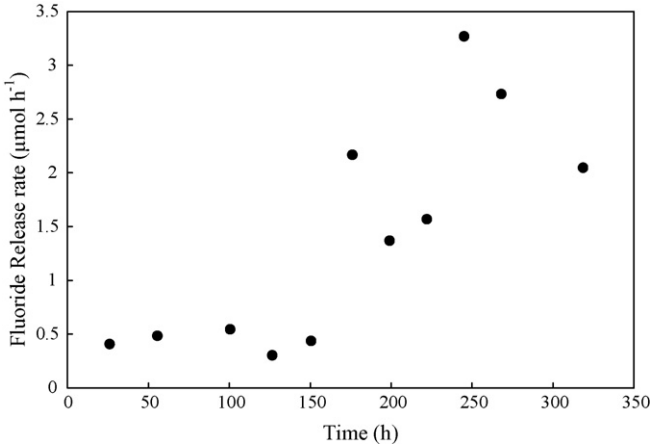

Fig. 7. Fluoride release rate over the testing period.

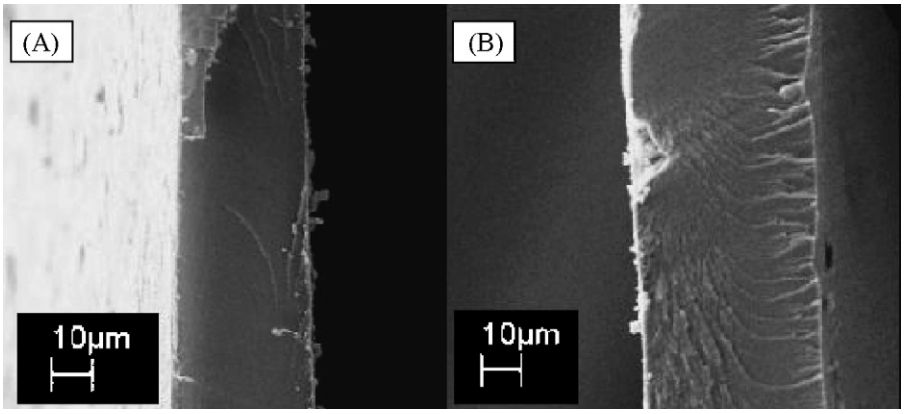

Fig. 8. SEM cross-sections of (A) un-degraded and (B) degraded membrane.

3.3. Fluoride release rate behaviour

Fluoride release behaviour of the fuel cell was also monitored over the testing period and the results are plotted in Fig. 7. Despite some outliers, the fluoride release rate in the period from 0 h to 150 h had an average rate of 0.72 μmol h^{-1} which was lower than the release rate from 150 h to 300 h, averaging 1.99 μmol h^{-1}. This is consistent with the mechanism of fluoride release whereby crossover of hydrogen or oxygen will react to form peroxide species, which will then degrade the polymer electrolyte membrane and produce fluoride ions. Thus, an increase in permeability and crossover rates will increase the fluoride release emissions. The variability in the rate data is attributed to cell start-up phenomena after the measurement of crossover and polarization curves.

3.4. Scanning electron microscopy results

Scanning electron microscopy imaging of the membrane was performed after the durability experiment had concluded to determine the extent of membrane thinning and to identify integrity failures. Prior to imaging, the gas diffusion electrode was removed from the polymer electrolyte to facilitate imaging of the polymer surface. In general, the membrane was intact with the exception of several tears and holes. Comparison of cross-sectional images from a fresh and the aged membrane, Fig. 8, revealed that there was no membrane thinning over the course of the experiment, however, cross-sections of the most obviously degraded regions could not be done due to the fragile nature of the membrane in those specific sections. Thus, though the membrane may have thinned locally, there was little overall thinning. Images of the surface revealed holes and tears as shown in Fig. 9. The SEM findings are consistent with the interpretation of the gas selectivity data.

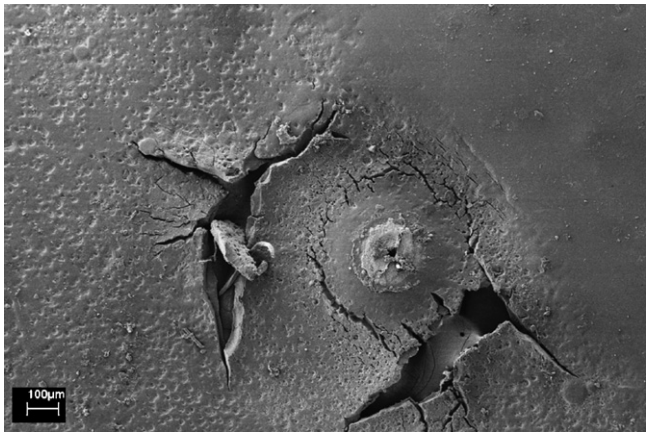

Fig. 9. SEM image of an integrity failure, tear, on the de-catalyzed degraded membrane.

4. Conclusions

This work proposes the use of gas selectivity measurements as a new diagnostic tool for fuel cell durability work. With the use of permeability and selectivity measurements for different gasses it is possible to distinguish between membrane thinning, and the onset of integrity failures in a membrane electrode assembly. Thinning phenomena is considered to have no impact on gas selectivity of the electrolyte membrane while still allowing gas crossover and apparent permeability to increase. The presence of holes and defects however will shift the permeability characteristics from solution diffusion behaviour through the electrolyte to Knudsen behaviour.

Through the use of gas crossover measurements of five gasses (H_2, N_2, He, O_2, Ar) across a fuel cell membrane electrode assembly subjected to an open circuit voltage (OCV) durability experiment, and subsequent calculation of permeability and selectivity, it was shown that the onset of a mechanical failure could be identified. Overall, with degradation the apparent permeability of gasses through the MEA increased exponentially. The results showed that with extended operation at OCV gas permeation behaviour changed from one characterized by solution diffusion behaviour (indicating that the polymer electrolyte membrane was defect free and therefore controlling the permeation rate) to one that followed Knudsen behaviour (indicating that defects had formed in the membrane and the catalyst/gas diffusion layer was controlling permeation rates). Plots of selectivity versus time showed that immediately from the start of the durability experiment the membrane showed changing selectivity which indicates that there was little membrane thinning and most of the increased apparent permeability was due to the appearance of integrity failures.

The change from solution diffusion behaviour to Knudsen behaviour, defect free to that with integrity failures, coincided with an increase in the voltage degradation rate and a significant drop in performance as shown by polarization curve measurements. Furthermore, the rate of fluoride ion release increased after the formation of integrity defects, which is consistent with observations of increasing crossover rates. Examination of the de-catalyzed membrane with scanning electron microscopy revealed rips and tears in the membrane confirming the interpretation of selectivity results. Comparison of cross-sections from fresh and aged membranes showed little generalized membrane thinning which was consistent with the selectivity data.

Acknowledgement

The authors would like to acknowledge the Natural Sciences and Engineering Research Council (NSERC) of Canada for financial support.

References

[1] A.B. LaConti, M. Hamdan, R.C. McDonald, in: W. Vielstich, H. Gasteiger, A. Lamm (Eds.), Handbook of Fuel Cells—Fundamentals, Technology and Applications, vol. 3, John Wiley & Sons, New York, 2003, pp. 647–663.
[2] S. Kundu, M.W. Fowler, L.C. Simon, S. Grot, J. Power Sources 157 (2006) 650–656.
[3] Q. Guo, Z. Qi, J. Power Sources 160 (2006) 1269–1274.
[4] E. Endoh, S. Terazono, H. Widjaja, Y. Takimoto, Electrochem. Solid-State Lett. 7 (2004) A209–A211.
[5] J. St Pierre, D.P. Wilkinson, S. Knights, M.L. Bos, J. New Mater. Electrochem. Syst. 3 (2000) 99–106.
[6] M.F. Mathias, R. Makharia, H.A. Gasteiger, J.J. Conley, T.J. Fuller, C.J. Gittleman, S.S. Kocha, D.P. Miller, C.K. Mittelsteadt, T. Xie, S.G. Yan, P.T. Yu, Electrochem. Soc. Interface 14 (2005) 24–36.
[7] J. Healy, C. Hayden, T. Xie, K. Olson, R. Waldo, H. Gasteiger, J. Abbott, Fuel Cells 5 (2005) 302–308.
[8] T. Kinumoto, M. Inaba, Y. Nakayama, K. Ogata, R. Umebayashi, A. Tasaka, Y. Iriyama, T. Abe, Z. Ogumi, J. Power Sources 158 (2006) 1222–1228.
[9] S. Kundu, L.C. Simon, M. Fowler, S. Grot, Polymer 46 (2005) 11707–11715.
[10] Y. Tang, M.H. Santare, A.M. Karlsson, S. Cleghorn, W.B. Johnson, J. Fuel Cell Sci. Technol. 3 (2006) 119–124.
[11] H. Liu, J. Zhang, F.D. Coms, W. Gu, B. Litteer, H.A. Gasteiger, ECS Trans. 3 (2006) 493–505.
[12] A. Ohma, S. Suga, S. Yamamoto, K. Shinohara, ECS Trans. 3 (2006) 519–529.
[13] M. Inaba, 14th International Conference on the Properties of Water and Steam, Kyoto, 2005, pp. 395–402.
[14] C.H. Paik, T. Skiba, V. Mittal, S. Motupally, T.D. Jarvi, 207th Meeting of the Electrochemical Society—Meeting Abstracts, 2005, p. 771.
[15] S. Kundu, L.C. Simon, M.W. Fowler, Polym. Degrad. Stab. 93 (2008) 214–224.
[16] X. Cheng, J.L. Zhang, Y.H. Tang, C.J. Song, J. Shen, D.T. Song, J.J. Zhang, J. Power Sources 167 (2007) 25–31.
[17] P. Pandey, R.S. Chauhan, Prog. Polym. Sci. 26 (2001) 853–893.
[18] J.S. Chiou, D.R. Paul, Ind. Eng. Chem. Res. 27 (1988) 2161–2164.
[19] S. Takahashi, M. Yoshida, M. Asano, T. Tanaka, T. Nakagawa, J. Appl. Polym. Sci. 82 (2001) 206–216.
[20] Z. Benjelloun-Dabaghi, A. Benali, Oil Gas Sci. Technol. 56 (2001) 295–303.
[21] A.E. Yaroshehuk, J. Membr. Sci. 101 (1995) 83–87.